2009 American Control Conference
Hyatt Regency Riverfront, St. Louis, MO, USA
June 10-12, 2009

Nonlinear Control of Non-minimum Phase Hypersonic Vehicle Models

Lisa Fiorentini*
Andrea Serrani
The Ohio State University
Columbus, OH 43210, USA

Michael A. Bolender
David B. Doman
U.S. Air Force Research Laboratory
Wright-Patterson AFB, OH 45433, USA

Abstract— **Longitudinal rigid-body models of air-breathing hypersonic vehicle dynamics are characterized by exponentially unstable zero-dynamics when longitudinal velocity and flight-path angle (FPA) are selected as regulated output. To enable application of stable dynamic inversion methods (and their adaptive counterparts), previous studies have considered the addition of a canard control surface to eliminate the occurrence of the unstable zero; however, the addition of a canard may negatively impact the design of the thermal protection system. In this paper, we present a methodology for robust nonlinear control of the rigid-body longitudinal hypersonic vehicle dynamics which employs only the elevator as aerodynamic control surface. The method reposes upon a nonlinear transformation of the equations-of-motion into the interconnection of systems in so-called feedback and feed-forward forms that allows the combination of high-gain and low-amplitude feedback, achieved through the use of saturated functions. Simulation results using the flexible vehicle model are presented to illustrate the effectiveness of the method.**

I. Introduction

One of the most severe challenges encountered in designing flight control systems for air-breathing hypersonic vehicle models, is the exponentially non-minimum phase behavior exhibited by the rigid-body flight-path angle (FPA) dynamics. This non-minimum phase behavior, which manifests itself as a hyperbolic saddle equilibrium in the pitch dynamics, arises [1] as a consequence of elevator-to-lift coupling. The unstable zero limits considerably the achievable bandwidth of the FPA loop, with negative repercussions for robust stability margins when designing linear control systems. For nonlinear control design, the presence of unstable zero-dynamics is a serious roadblock, as it prevents the application of standard dynamic inversion methods. In [2], approximate feedback linearization was applied to the model of Bolender and Doman [3] by strategically ignoring the elevator-to-lift coupling, thereby artificially extending the relative degree between FPA and elevator deflection from one to three and removing the presence of the zero from the model. In the same work, as also initially suggested in [1], a canard was added to the control suite to counteract the non-minimum phase behavior by ganging the canard and the elevator deflection via a constant gain. The availability of an additional control surface was heavily exploited in subsequent nonlinear adaptive control design [4]–[6], where the elevator-to-lift coupling was adaptively canceled. The resulting closed-loop system was proved in [5], [6] to be robust with respect to the dynamic uncertainty given by the aero-elastic dynamics. The presence of a canard, while beneficial for controllability, may negatively impact the design of the thermal protection system, as this additional control surface must withstand a significant thermal stress. Consequently, for hypersonic vehicles it is of interest to investigate methodologies for nonlinear control design under the assumption that the elevator is the only aerodynamic control surface available for the longitudinal dynamics.

In this paper, we apply a methodology strongly inspired by the results in [7], which uses a preliminary feedback transformation to convert the FPA and pitch dynamics into the interconnection of a system in feed-forward form and a system in feedback form, respectively. Then, a combination of adaptive, high-gain and low-amplitude feedback, achieved through the use of saturation design and input-to-state stability methods [8], [9], is employed. Since the focus of the paper is on counteracting the exponentially non-minimum phase behavior of the rigid-body FPA dynamics, only the rigid-body control-oriented vehicle model considered in [4] is used for controller design and stability analysis. However, the full nonlinear model in [3], which includes structural flexibility, is employed for closed-loop simulations.

The paper is organized as follows: in Section II the vehicle model is introduced and the control objective is stated. Section III elaborates on the system zero-dynamics, while in section IV the control design is presented together with the stability analysis. Finally, simulation results are discussed in Section V, and conclusions are offered in Section VI.

II. Vehicle Model

The rigid-body vehicle dynamics considered in this study is given as follows [3]

$$\begin{aligned} \dot{V} &= \frac{T\cos\alpha - D}{m} - g\sin\gamma \qquad \dot{\theta} = Q \\ \dot{\gamma} &= \frac{L + T\sin\alpha}{mV} - \frac{g}{V}\cos\gamma \qquad \dot{Q} = \frac{M}{I_{yy}} \end{aligned} \tag{1}$$

This model comprises four rigid-body state variables $x = [V, \gamma, \theta, Q]^T$ and two control inputs $u = [\Phi, \delta_e]^T$ which affect (1) through the thrust, T, the pitching moment about the body y-axis, M, lift, L, and drag, D. The output to be controlled is selected as $y = [V, \gamma]^T$. The meaning of the state variables and the input vector is given in Table I. Following [2], approximations of the forces and moments to

*Corresponding author, Department of Electrical and Computer Engineering, The Ohio State University, 2015 Neil Ave, Columbus, OH. Email: fiorentini.2@osu.edu

TABLE I

ADMISSIBLE RANGES FOR STATE, INPUT, AND VARIABLES OF INTEREST

Var		Min Value	Max Value
V	Vehicle Velocity	7500 ft/s	11000 ft/s
γ	Flight-Path Angle (FPA)	-3 deg	3 deg
θ	Pitch Angle	-5 deg	5 deg
Q	Pitch Rate	-10 deg/s	10 deg/s
Φ	Fuel-to-air Ratio	0.05	1.5
δ_e	Elevator Deflection	-20 deg	20 deg
h	Vehicle Altitude $\dot{h} = V \sin\gamma$	85000 ft	135000 ft
α	Angle-of-Attack, $\alpha = \theta - \gamma$	-5 deg	5 deg
$\bar{q}$	Dynamic Pressure	182.5 psf	2200 psf

be employed for control design and stability analysis have been derived as follows:

$$\begin{aligned} T &\approx T(\alpha,\Phi) \\ L &\approx \bar{q}S\big[C_L^{\alpha}\alpha + C_L^0 + C_L^{\delta}\delta_e\big] \\ D &\approx \bar{q}S\big[C_D^{\alpha^2}\alpha^2 + C_D^{\alpha}\alpha + C_D^0 + C_D^{\delta^2}\delta_e^2 + C_D^{\delta}\delta_e\big] \\ M &\approx z_T T(\alpha,\Phi) + \bar{q}\bar{c}\,S\big[C_M^{\alpha}\alpha + C_M^0 + C_M^{\delta}\delta_e\big] \end{aligned} \tag{2}$$

where $T(\alpha,\Phi)$ is a continuously differentiable bounded function of α for any given Φ. As a consequence, one can write $T(\alpha,\Phi) = \Delta T(\alpha,\Phi)\alpha + T(0,\Phi)$. Note that Φ is physically limited to take values within the ranges of Table I. The goal pursued in this study is to design a state-feedback controller to steer the state of system (1) from a given compact set of initial conditions, $x_0 = [V_0, \gamma_0, \theta_0, Q_0]^T \in \Xi_0$, to a desired trim condition $x^\star = [V^\star, 0, \theta^\star, 0]^T$, along smooth exogenous reference trajectories $y_{\rm ref}(t) = [V_{\rm ref}(t),\ \gamma_{\rm ref}(t)]^T$. The velocity and FPA references are generated by the guidance subsystem to satisfy the bounds shown in Table I, which determine the considered flight envelope of the vehicle. The set Ξ_0 is also assumed to be a subset of the set in Table I. Clearly, $\lim_{t\to\infty} V_{\rm ref}(t) = V^\star$ and $\lim_{t\to\infty}\gamma_{\rm ref}(t) = 0$. It should be noted that in reality, once a desired trim condition $V^\star$ is reached, neither $\theta^\star$ or the value of the control input at trim, $u^\star = [\Phi^\star, \delta_e^\star]^T$, can be determined a priori due to parameter uncertainty. In this preliminary study the presence of model uncertainty is not directly addressed, but is implicitly treated as a disturbance on the nominal model. Integral action provided by the controller is used to overcome the effect of residual terms when applying dynamics inversion (note that θ^* is assumed to be unknown). As a result, the control requirement is posed as that of designing a controller such that, in a suitable set of coordinates, the dynamics of the tracking error in closed-loop are input-to-state stable with respect to external disturbances.

III. THE ZERO-DYNAMICS OF HSVS

It is apparent that the model (1) has vector relative degree $r = [1,1]$ with respect to the regulated output. As a result, the systems has a 2-dim zero-dynamics with respect to the set-point error $e = [V - V^\star, \gamma]^T$. For ease of notation, let

$$\bar{C}_M^{\delta} := -\frac{C_M^{\delta}}{C_L^{\delta}}, \quad \bar{z}_T(\alpha) := z_T + \bar{c}\,\bar{C}_M^{\delta}\sin\alpha$$
$$\bar{C}_M^{\alpha}(\alpha) := C_M^{\alpha}(\alpha) + \bar{C}_M^{\delta}C_L^{\alpha}(\alpha) - \bar{C}_M^{\delta}\tfrac{mg}{\bar{q}S}$$

and define the *effective moment* $\bar{M}(\alpha,\Phi) = \bar{c}\,\bar{q}S\,\bar{C}_M^{\alpha}(\alpha) + \bar{z}_T(\alpha)T(\alpha,\Phi)$ Applying the *decoupling control input*

$$\delta_e^\star(\alpha,\Phi,\gamma) := \frac{1}{\bar{q}SC_L^{\delta}}\big[-\bar{q}SC_L^{\alpha}(\alpha) - T(\alpha,\Phi)\sin\alpha + mg\cos\gamma\big]$$

and choosing the initial condition $\gamma(0) = 0$, one obtains the zero dynamics of the system (1) (with respect to the output γ)

$$\begin{aligned} \dot{\theta} &= Q \\ I_{yy}\dot{Q} &= \bar{M}(\theta,\Phi) \end{aligned} \tag{3}$$

where we have use the fact that $\gamma = 0$ implies $\alpha = \theta$. Note that in equation (3), Φ is regarded as a time-varying parameter. System (3) has an equilibrium at $(\theta, Q) = (\theta^\star, 0)$ and $\Phi = \Phi^\star$, where the constant values $\theta^\star$, $\Phi^\star$ are determined by the trim condition at $V = V^\star$, namely

$$\begin{aligned} T(\theta^\star,\Phi^\star)\cos\theta^\star - D\big(\theta^\star, \delta_e^\star(\theta^\star,\Phi^\star,0)\big) &= 0 \\ \bar{M}(\theta^\star,\Phi^\star) &= 0 \end{aligned} \tag{4}$$

Since it can be verified that $\frac{\partial\bar{M}(\theta,\Phi)}{\partial\theta}|_{\substack{\theta=\theta^\star \\ \Phi=\Phi^\star}} > 0$ for the considered flight envelope, it follows that the equilibrium $(\theta, Q) = (\theta^\star, 0)$ of the pitch dynamics (3) is a hyperbolic saddle. As a result, any attempt to apply a standard dynamic inversion algorithm to the relative-degree $r = [1,1]^T$-system (1) results in unstable internal dynamics.

IV. CONTROL DESIGN

Given the reference $V_{\rm ref}(t)$ and $\gamma_{\rm ref}(t)$ the corresponding tracking errors are defined as $\tilde{V} = V - V_{\rm ref}$ and $\tilde{\gamma} = \gamma - \gamma_{\rm ref}$. The velocity subsystem is controlled using thrust from the fuel equivalence ratio, Φ. The pitch angle is used as a virtual input to control the FPA by defining a suitable bounded commanded reference $\theta_{\rm cmd}$. Finally, the control law for the elevator deflection is derived using dynamic inversion to control the rotational dynamics through the pitch moment.

A. Velocity Subsystem

In the error coordinate, the first equation of (1) reads as

$$\dot{\tilde{V}} = \frac{T\cos\alpha - D}{m} - g\sin\gamma - \dot{V}_{\rm ref}\,. \tag{5}$$

Since the thrust can be approximated locally as $T(\alpha,\Phi) \approx \bar{q}S\big[C_T^{\Phi\alpha^3}\alpha^3 + C_T^{\Phi\alpha^2}\alpha^2 + C_T^{\Phi\alpha}\alpha + C_T^{\Phi} + C_T^3\alpha^3 + C_T^2\alpha^2 + C_T^1\alpha + C_T^0\big]$, Eq. (5) can be written as

$$m\dot{\tilde{V}} \;=\; \vartheta^T B(\alpha)\Phi - \Psi^T(x,u)\,\vartheta$$

by introducing the vector of uncertain parameters ϑ, the regressor Ψ and the input matrix B respectively as

$$\begin{aligned} \vartheta &= S\,[C_T^{\Phi\alpha^3}, C_T^{\Phi\alpha^2}, C_T^{\Phi\alpha}, C_T^{\Phi}, C_T^3, C_T^2, C_T^1, C_T^0, \\ &\qquad C_D^{\alpha^2}, C_D^{\alpha}, C_D^0, C_D^{\delta_e^2}, C_D^{\delta_e}, m/S]^T \\ \Psi(x,u) &= [0_{1\times4}, -\bar{q}\alpha^3\cos\alpha, -\bar{q}\alpha^2\cos\alpha, -\bar{q}\alpha\cos\alpha, \\ &\qquad -\bar{q}\cos\alpha, \bar{q}\alpha^2, \bar{q}\alpha\,, \bar{q}\,, \bar{q}\delta_e^2, \bar{q}\delta_e, g\sin\gamma + \dot{V}_{\rm ref}]^T \\ B(\alpha) &= \bar{q}\,[\alpha^3\cos\alpha, \alpha^2\cos\alpha, \alpha\cos\alpha, \cos\alpha, 0_{1\times10},]^T. \end{aligned}$$

Let $\hat{\vartheta}$ be a vector of estimates of ϑ and Θ be the compact set in which $\hat{\vartheta}$ is assumed to range. Following [4], the control law for the equivalence air ratio is chosen as

$$\Phi \;=\; \frac{1}{\hat{\vartheta}^T B(\alpha)} \left[-k_V \tilde{V} + \Psi^T(x,u)\,\hat{\vartheta} \right]$$

where $k_V > 0$ is a gain parameter. Consequently, the update law for the parameter estimate $\hat{\vartheta}$ is chosen as

$$\dot{\hat{\vartheta}} = \underset{\vartheta \in \Theta}{\mathrm{Proj}} \left\{ \tilde{V}\,\Gamma \left[B(\alpha,\bar{q})\Phi - \Psi(x,u,y_{\mathrm{ref}}) \right] \right\}$$

where $\Gamma \in \mathbb{R}^{14\times 14}$ is a symmetric positive definite matrix and $\mathrm{Proj}_{\vartheta\in\Theta}$ is a smooth parameter projection [10]. Using a suitable Lyapunov function it is possible to prove that as long as the trajectories of the overall system are defined, the velocity tracking error converges asymptotically to zero while the parameter estimates remain bounded.

B. FPA and Pitch Dynamics

Since a form of dynamic inversion will be applied, the FPA/Pitch dynamics are augmented with an integrator to deal with model uncertainties. This ensures that at any trim condition x^*, necessarily $\tilde{\gamma}^* = 0$. The elevator deflection control law is chosen as

$$\delta_e = \frac{1}{C_M^\delta} \left[\frac{I_{yy}}{\bar{q}\bar{c}S}\, v - C_M^\alpha \alpha - C_M^0 - \frac{z_T}{\bar{q}\bar{c}S} T \right]$$

where v is an additional control input to be designed. As a result, the rotational dynamics read as

$$\begin{aligned} \dot{\zeta} &= \tilde{\gamma} & \dot{\theta} &= Q \\ \dot{\tilde{\gamma}} &= \varphi_1(x,\phi)\,\alpha - \varphi_2(x)\,v + d & \dot{Q} &= v \end{aligned} \tag{6}$$

where

$$\varphi_1(x,\phi) := \frac{\bar{q}S}{mV}\left(C_L^\alpha - \frac{C_L^\delta C_M^\alpha}{C_M^\delta} \right) + \frac{T}{mV}\frac{\sin\alpha}{\alpha} - \frac{z_T C_L^\delta}{\bar{c}\, C_M^\delta}\frac{\Delta T(\alpha,\Phi)}{mV}$$

$$\varphi_2(x) := -\frac{1}{mV}\,\frac{I_{yy} C_L^\delta}{\bar{c}\, C_M^\delta} \tag{7}$$

$$d := \frac{\bar{q}S}{mV}\left(C_L^0 - \frac{C_L^\delta C_M^0}{C_M^\delta} \right) - \frac{z_T\, C_L^\delta}{\bar{c}\, C_M^\delta}\frac{T(0,\Phi)}{mV} \tag{8}$$

$$- \frac{g}{V}\cos\gamma - \dot{\gamma}_{\mathrm{ref}}. \tag{9}$$

Using similar arguments to the ones used in [4], it is possible to show that there exist positive coefficient φ_1^M and φ_1^m such that $\varphi_1^m < \varphi_1(x,\phi) < \varphi_1^M$. Moreover, for the envelope of flight conditions considered in Table I, there exist positive coefficients φ_2^m, and φ_2^M, such that $\varphi_2^m < \varphi_2(x) < \varphi_2^M$.

The (θ, Q)-subsystem will be used as a servo-loop for controlling the FPA by properly defining a bounded command θ_{cmd}. In particular, a two-time scale behavior will be enforced in the rotational dynamics by applying high-gain feedback to the inner loop represented by the (θ, Q)-subsystem, low-gain feedback to the outer loop, i.e., the $(\zeta, \tilde{\gamma})$-subsystem, and by exploiting properties of saturated interconnections. Let $\sigma : \mathbb{R} \to \mathbb{R}$ be a differentiable function which satisfies the following properties

$$\begin{aligned} &|\sigma'(s)| := |\mathrm{d}\sigma(s)/\mathrm{d}s| \le 2 \quad \text{for all } s \\ &s\sigma(s) > 0 \quad \text{for all } s \neq 0\,,\ \sigma(0) = 0 \\ &\sigma(s) = \mathrm{sgn}(s) \ \text{ for } |s| \ge 1 \\ &|s| < |\sigma(s)| < 1 \ \text{ for } |s| < 1 \end{aligned} \tag{10}$$

Similarly to what done in [7], the following nonlinear change of coordinates is applied to system (6)

$$\begin{aligned} \xi_1 &= \zeta \\ \xi_2 &= \tilde{\gamma} + \lambda_1\, \sigma\!\left(\frac{k_1 \xi_1}{\lambda_1} \right) \\ \eta_1 &= \theta - \theta_{\mathrm{cmd}} \\ \eta_2 &= Q + k_P \left(\theta - \theta_{\mathrm{cmd}} \right) \end{aligned}$$

and v and θ_{cmd} are chosen as

$$v = -(k_P + k_D)\,\eta_2 + (k_D^2 - 1)\,\eta_1$$

$$\theta_{\mathrm{cmd}} = \gamma_{\mathrm{ref}} - \lambda_1\, \sigma\!\left(\frac{k_1 \xi_1}{\lambda_1} \right)$$

where k_1 and λ_1 are positive design parameters and k_P and k_D are respectively proportional and derivative gains. Recalling that $\alpha = \theta - \tilde{\gamma} - \gamma_{\mathrm{ref}}$, in the new coordinates system (6) reads as

$$\dot{\xi}_1 = -\lambda_1\, \sigma\!\left(\frac{k_1 \xi_1}{\lambda_1} \right) + y_z \tag{11}$$

$$\dot{\xi}_2 = -\left[\varphi_1(x,\phi) - k_1 \sigma'\!\left(\frac{k_1 \xi_1}{\lambda_1} \right) \right] \xi_2 + y_\eta + y_{\xi_1} + d \tag{12}$$

$$\dot{\eta}_1 = -k_P \eta_1 + \eta_2 + y_{\xi_1} + y_{\xi_2} - \dot{\gamma}_{\mathrm{ref}}$$

$$\dot{\eta}_2 = -k_D \eta_2 - \eta_1 + k_P y_{\xi_1} + k_P y_{\xi_2} - k_P \dot{\gamma}_{\mathrm{ref}} \tag{13}$$

$$y_{\xi_1} = -\lambda_1 k_1 \sigma'\!\left(\frac{k_1 \xi_1}{\lambda_1} \right) \sigma\!\left(\frac{k_1 \xi_1}{\lambda_1} \right) \tag{14}$$

$$y_{\xi_2} = k_1 \sigma'\!\left(\frac{k_1 \xi_1}{\lambda_1} \right) \xi_2 \tag{15}$$

$$y_z = \xi_2 \tag{16}$$

$$y_\eta = \left[\varphi_1(x,\phi) - \varphi_2(x)(k_D^2 - 1) \right] \eta_1 + \varphi_2(x)(k_P + k_D)\,\eta_2\,. \tag{17}$$

Let $\xi = [\xi_1, \xi_2]^T$, $\eta = [\eta_1, \eta_2]^T$ and $z := [\xi_2, \eta]^T$. Fix $k_D > 0$, $k_P > 0$ and let $k_1 := k_1^* \varepsilon$, where k_1^* is a positive real number and ε is a positive design parameter. In particular, ε will be tuned to render the ξ-dynamics sufficiently slower than the η-dynamics. The use of the saturation function allows the command θ_{cmd} to remain bounded even when the norm of the state of the slower dynamics becomes large.

The first step in the stability analysis is to show that the (ξ, η)-system defined by (11)-(17) is input-to-state stable (ISS), with no restriction on the initial state and restrictions on the input d. To this aim, the asymptotic properties[1] of the ξ_2 and η-subsystems will be first analyzed separately. It will be shown that the interconnection of the ξ_2 and η-subsystems

[1] In the following, we use the notation adopted in [9]

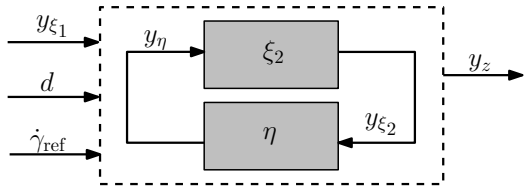

Fig. 1. Interconnection of the ξ_2 and η subsystems.

(see Figure 1) is ISS, with no restriction on the initial state and on the inputs $(y_{\xi_1}, d, \dot\gamma_{\rm ref})$. Then, the asymptotic properties of the ξ_1-subsystem will be considered, and the interconnection of the z-subsystem and ξ_1-subsystem (see Figure 2) will be analyzed. The following two propositions establish the asymptotic bounds on the ξ_2 and η trajectories.

Proposition 4.1: Consider system (12) with output (15). There exists $\varepsilon_1^* > 0$ such that for all $\varepsilon < \varepsilon_1^*$ this system is ISS without restriction on the initial state and on the inputs (y_η, y_{ξ_1}, d). Moreover, the output y_{ξ_2} satisfies

$$\|y_{\xi_2}\|_a < \frac{6\,k_1}{\varphi_1^m - 2k_1}\ \max\{\,\|y_\eta\|_a,\ \|y_{\xi_1}\|_a,\ \|d\|_a\}\,. \quad (18)$$

Proof: Let us consider the Lyapunov function candidate $W_1(\xi_2) = \frac{1}{2}\,\xi_2^2$, and let $\varepsilon_1^* = \varphi_1^m/(2k_1^*)$. The derivative of W_1 along trajectories of system (12) satisfies

$$\dot W_1 < -(\varphi_1^m - 2k_1)\,\xi_2^2 + |\xi_2|\,\big(|y_\eta| + |y_{\xi_1}| + |d|\big)$$

therefore, for $\varepsilon < \varepsilon_1^*$ (recall that $k_1 = \varepsilon k_1^*$)

$$|\xi_2| > \frac{3}{\varphi_1^m - 2k_1}\ \max\{\,|y_\eta|,\ |y_{\xi_1}|,\ |d|\} \ \ \Rightarrow\ \ \dot W_1 < 0\,.$$

As a result, W_1 is an ISS Lyapunov function for system (12), hence (see [9, Lemma 3.3])

$$\|\xi_2\|_a < \frac{3}{\varphi_1^m - 2k_1}\ \max\{\,\|y_\eta\|_a,\ \|y_{\xi_1}\|_a,\ \|d\|_a\}\,. \quad (19)$$

Using (10) it follows that $|y_{\xi_2}| \le 2k_1|\xi_2|$, therefore the asymptotic bound on y_{ξ_2} is readily obtained from (19). ■

Proposition 4.2: For any $k_P, k_D > 0$, the system (13) with output (17) is ISS without restriction on the initial state and on the inputs $(y_{\xi_1}, y_{\xi_2}, \dot\gamma_{\rm ref})$. Moreover, the output y_η satisfies the asymptotic bound

$$\|y_\eta\|_a < a_1 \max\{\,\|y_{\xi_1}\|_a\,,\ \|y_{\xi_2}\|_a\} \quad (20)$$

where a_1 is a positive constant that depends on k_P and k_D.

Proof: The derivative of the Lyapunov function candidate $W_2(\eta_1,\eta_2) = \frac{1}{2}\eta_1^2 + \frac{1}{2}\eta_2^2$ along trajectories of system (13) satisfies

$$\begin{aligned}\dot W_2 &\le -k_P\eta_1^2 - k_D\eta_2^2 + (|\eta_1| + k_P|\eta_2|)\big(|y_{\xi_1}| + |y_{\xi_2}| + |\dot\gamma_{\rm ref}|\big)\\ &\le -c\|\eta\|^2 + 2(1+k_P)\|\eta\|\big(|y_{\xi_1}| + |y_{\xi_2}| + |\dot\gamma_{\rm ref}|\big)\end{aligned}$$

where $c := \min\{k_D, k_P\}$. Then,

$$\|\eta\| > \frac{6(1+k_P)}{c}\max\{\,|y_{\xi_1}|\,,\ |y_{\xi_2}|\,,\ |\dot\gamma_{\rm ref}|\} \ \ \Rightarrow\ \ \dot W_2 < 0\,.$$

As a result, W_2 is an ISS Lyapunov function for system (13) and therefore the latter is ISS without restriction on the initial state and on the inputs $(y_{\xi_1}, y_{\xi_2}, \dot\gamma_{\rm ref})$. Since $\lim_{t\to\infty}\dot\gamma_{\rm ref}(t) = 0$,

$$\|\eta\|_a < \frac{6(1+k_P)}{c}\max\{\,\|y_{\xi_1}\|_a,\ \|y_{\xi_2}\|_a\}\,. \quad (21)$$

Considering (17), the asymptotic bound on y_η holds with

$a_1 := \frac{6(1+k_P)}{c}\max\{\varphi_1^M + \varphi_2^M|k_D^2 - 1|, \varphi_2^M(k_P + k_D)\}$. ■

Now we consider the interconnection depicted in Figure 1:

Proposition 4.3: There exists a number $\varepsilon_3^* > 0$ such that for all $\varepsilon < \varepsilon_3^*$ the interconnection of systems (12) and (13) is ISS without restriction on the initial state and on the inputs $(y_{\xi_1}, d, \dot\gamma_{\rm ref})$. Moreover, y_z satisfies the asymptotic bound

$$\|y_z\|_a < \frac{3}{\varphi_1^m - 2k_1}\ \max\{\,a_2\,\|y_{\xi_1}\|_a,\ \|d\|_a\} \quad (22)$$

where a_2 is a positive coefficient that does not depend on ε.

Proof: Using Propositions (4.1) and (4.2), it follows that for any $\varepsilon < \varepsilon_1^*$ the asymptotic bounds (18) and (20) hold. Let $\varepsilon_2^* = \varphi_1^m/(6a_1+2)k_1^*$. Then for any $\varepsilon < \varepsilon_3^* := \min\{\varepsilon_1^*, \varepsilon_2^*\}$ the small-gain condition

$$\frac{6\,k_1}{\varphi_1^m - 2k_1}\ \cdot a_1 < 1\,. \quad (23)$$

holds, and thus the interconnection is ISS by virtue of [9, Theorem 1], and

$$\begin{aligned}\|y_{\xi_2}\|_a &< \frac{6k_1}{\varphi_1^m - 2k_1}\max\{\,a_2\|y_{\xi_1}\|_a,\ \|d\|_a\}\\ \|y_\eta\|_a &< a_1\max\{\,a_3(\varepsilon)\,\|y_{\xi_1}\|_a\,, \frac{6k_1}{\varphi_1^m - 2k_1}\,\|d\|_a\} \quad (24)\end{aligned}$$

where $a_2 := \max\big\{a_1, 1\big\}$, $a_3(\varepsilon) := \max\big\{6k_1/(\varphi_1^m - 2k_1), 1\big\}$. Since $y_z = \xi_2$, the bound (22) follows by combining (19) with (24) and using (23). ■

Finally, the following proposition holds for the ξ_1-subsystem:

Proposition 4.4: System (11) is ISS without restriction on the initial state and restriction λ_1 on the input y_z, and its output (14) satisfies

$$\|y_{\xi_1}\|_a < 2k_1\,\|y_z\|_a\,.$$

Proof: Since the right hand side of Eq. (11) is globally Lipschitz, the ξ_1-trajectories are defined for any $t \ge 0$ for any locally essentially bounded input $y_z(\cdot)$. Consequently, if $y_z(\cdot)$ is such that $\sup_{t\in(t_1,\infty]}|y_z(t)| < \lambda_1$ for some $t_1 \ge 0$, from standard arguments it follows that $\exists\, t_2 > t_1$ such that $\sup_{t\in(t_2,\infty]}|\xi_1(t)| < \frac{1}{k_1}\sup_{t\in(t_2,\infty]}|y_z(t)| < \frac{\lambda_1}{k_1}$.

As a consequence $\|\xi_1\|_a < 1/k_1\ \|y_z\|_a$ and the result follows from the fact that $|y_{\xi_1}| \le 2k_1^2|\xi_1|$ when the saturation $\sigma(\cdot)$ is not active. ■

Next, it is verified that the restriction on y_z is met in finite time.

Proposition 4.5: Consider the z-subsystem in the interconnection depicted in Figure 2, driven by the output of system (11). There exist positive constants ε_4^* and λ_1^* such that for all $\varepsilon < \varepsilon_4^*$ and $\lambda_1 > \lambda_1^*$, $\|y_z\|_a < \lambda_1$. As a result, the restriction on the input for the upper subsystem (11) is met in finite time.

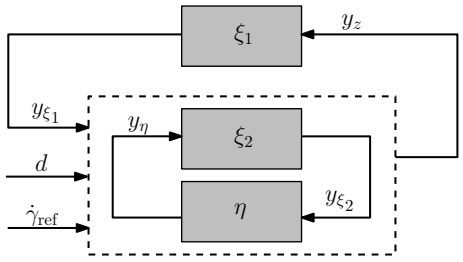

Fig. 2. Interconnection of the z and ξ_1 subsystems.

Proof: Let Δ be an upper bound for the $\mathcal{L}_\infty$-norm of the disturbance d in (7) (this bound exists since the velocity inner-loop ensures that V is bounded from below.) Define

$$\varepsilon_4^* := \min\left\{\frac{\varphi_1^m}{8k_1^*}\,,\,\varepsilon_2^*\right\} \quad \text{and} \quad \lambda_1^* := \frac{3\Delta}{\varphi_1^m - 2k_1^*\varepsilon_4^*}\,.$$

Then it can be verified that

$$\frac{3}{\varphi_1^m - 2k_1}\ \max\left\{\frac{a_1}{\sqrt{\varepsilon}},1\right\}\cdot 2k_1\lambda_1 < \lambda_1$$
$$\frac{3\Delta}{\varphi_1^m - 2k_1} < \lambda_1$$

for any $\varepsilon < \varepsilon_4^*$ and $\lambda_1 > \lambda_1^*$. The asymptotic bound on y_z follows from (22) by noticing that $\|y_{\xi_1}\|_\infty \le 2k_1\lambda_1$ and $\|d\|_\infty \le \Delta$. Since no finite escape time is possible in the overall system, we can conclude that there exists a positive time t_1 such that $\sup_{t\in(t_1,\infty]}|y_z(t)| < \lambda_1$ ■

The final step is to prove that the system in Figure 2 is a small-gain interconnection:

Proposition 4.6: Consider the overall system given by the interconnection of systems (12)-(13) and (11). Then for all $\varepsilon < \varepsilon_4^*$ this system is ISS without restriction on the initial state and restriction Δ on the input d, and its state satisfies the asymptotic bounds

$$\|\xi_1\|_a \le \frac{a_4(\varepsilon)}{k_1}\,\|d\|_a$$
$$\|\xi_2\|_a \le a_4(\varepsilon)\,\|d\|_a$$
$$\|\eta\|_a \le a_5(\varepsilon)\,\|d\|_a$$

where $a_4(\varepsilon)$ and $a_5(\varepsilon)$ are positive coefficients that depend on ε.

Proof: Recall that, by Propositions (4.3) and (4.4)

$$\|y_z\|_a < \frac{3}{\varphi_1^m - 2k_1}\ \max\{\,a_2\,\|y_{\xi_1}\|_a,\ \|d\|_a\}$$
$$\|y_{\xi_1}\|_a < 2k_1\,\|y_z\|_a\,.$$

Since it can be verified that

$$\frac{3\,a_2}{\varphi_1^m - 2k_1}\cdot 2k_1 \ <\ 1\,, \tag{25}$$

for $\varepsilon < \varepsilon_4^*$, by using small-gain arguments it follows that

$$\|\xi_2\|_a \ =\ \|y_z\|_a < \frac{3}{\varphi_1^m - 2k_1}\,\|d\|_a$$
$$\|\xi_1\|_a \ <\ \frac{1}{k_1}\,\|y_z\|_a < \frac{1}{k_1}\frac{3}{\varphi_1^m - 2k_1}\,\|d\|_a\,.$$

Applying properties (10) on (14) and (15) it follows that

$$\|y_{\xi_1}\|_a \ <\ 2k_1^2\,\|\xi_1\|_a < \frac{6k_1}{\varphi_1^m - 2k_1}\,\|d\|_a$$
$$\|y_{\xi_2}\|_a \ <\ 2k_1\,\|\xi_2\|_a < \frac{6k_1}{\varphi_1^m - 2k_1}\,\|d\|_a\,.$$

Finally, using (21) it follows that

$$\|\eta\|_a \ <\ \frac{6(1+k_P)}{c}\,\frac{6k_1}{\varphi_1^m - 2k_1}\,\|d\|_a$$

and therefore the proposition holds for

$$a_4(\varepsilon) := \frac{3}{\varphi_1^m - 2k_1}\,,\quad a_5(\varepsilon) := \frac{6(1+k_P)}{c}\,\frac{6k_1}{\varphi_1^m - 2k_1}\,.$$ ■

The result of Proposition 4.6 establishes, in particular, uniform ultimate boundedness of the tracking error with respect to the disturbance input d. If $\Phi(t)$ converges to a constant value, then the closed-loop system possesses an equilibrium in correspondence of the limit value d^*

$$d^* = \frac{\bar{q}S}{mV^*}\left(C_L^0 - \frac{C_L^\delta C_M^0}{C_M^\delta}\right) - \frac{z_T\,C_L^\delta}{\bar{c}\,C_M^\delta}\frac{T(0,\Phi)}{mV^*} - \frac{g}{V^*}\,.$$

Since we have augmented the FPA dynamics with an integrator, any equilibrium for system (6) satisfies necessarily $\tilde{\gamma}^* = 0$ and $Q^* = 0$. In the new coordinates this implies that

$$\xi_2^* - \lambda_1\sigma\left(\frac{k_1\xi_1^*}{\lambda_1}\right) = 0 \Rightarrow y_{\xi_1}^* + y_{\xi_1}^* = 0$$
$$\Rightarrow\ \ \eta_1^* = \eta_2^* = 0 \Rightarrow \xi_2^* = k_1\xi_1^* = \frac{d^*}{\varphi_1(x^*,\Phi^*)}\,.$$

It must be noted that, due to parameter and modeling uncertainties and the fact that dynamic inversion has been applied, the trim condition for the system is likely to be such that $(\eta_1^*,\eta_2^*) \neq (0,0)$. However, even in this case, the presence of the integrator still ensure that the condition $(\tilde{\gamma}^*,Q^*) = 0$ is guaranteed at trim. Indeed, this has been verified on the basis of nonlinear simulations conducted on the full nonlinear model, as described in the next section.

V. Simulations

To test the performance of controller derived in the previous section, simulations have been performed on the full nonlinear vehicle model described in [3], which includes structural flexibility. The vehicle is not trimmed at $t = 0$, $h(0) = 86000\,\text{ft}$ and $V(0) = 7850\,\text{ft/s}$. The velocity reference trajectory is generated to let the vehicle reach the desired final trim condition $V^* = 10500\,\text{ft/s}$. The flight path angle reference trajectory is generated filtering a step $s(t)$ such that, $s(t) = 5$ for $0 < t < 20$ and $s(t) = 0$ for $t \ge 20$, with a first-order pre-filter with natural frequency $\omega_f = 0.02$ rad/s and damping factor $\zeta_f = 0.95$. The controller gains have been chosen as $k_V = 120, k_P = 5, k_1 = 0.1, \Gamma_1 = 0.1\times I_{14\times 14}, k_D = 10, \lambda_1 = 0.041$. From Fig. 3(a)-(b) it is possible to see that since the vehicle in not trimmed at $t = 0$, the tracking errors in the initial interval of time are large, but the saturation function σ, allows the reference command θ_{cmd} to remain bounded and prevents the states to grow unbounded. In Fig. 3(a)-(c) typical nonlinear

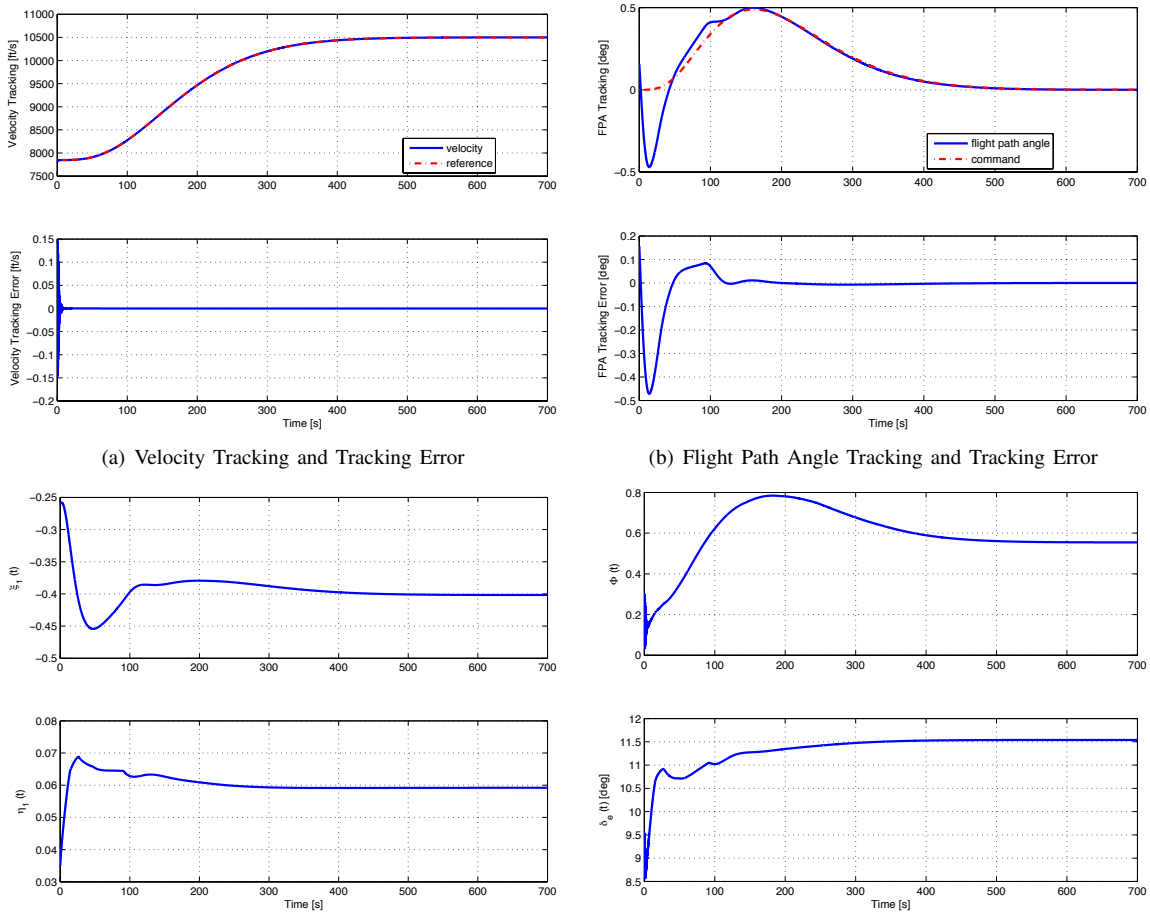

(a) Velocity Tracking and Tracking Error

(b) Flight Path Angle Tracking and Tracking Error

(c) Trajectories $\xi_1(t)$ and $\eta_1(t)$

(d) Control Inputs

Fig. 3. Simulation Results

phenomenon associated with the saturation are visible during the interval in which $\xi_1(t)$ is within the saturation limits. Eventually, the trajectory of the integrator enters the linear region of the saturation function, and the FPA tracking error converges to zero. As mentioned, the equilibrium does not satisfy the condition $\eta^* = 0$, however, the ξ and η variables are set to constant values that allow to reach the desired steady state trim condition $\gamma^* = 0$. Finally, Fig. 3(d) show that the control inputs remain well-behaved.

VI. Conclusions

In this paper, we have presented the application of methodologies based on small-gain theorems for saturated interconnections to the problem of controlling the longitudinal dynamics of hypersonic vehicle using only the elevator as aerodynamic control surface. The main focus of the paper is on counteracting the exponentially non-minimum phase behavior of the rigid-body FPA dynamics. While it has been shown in simulation that the method is effective on a more complex vehicle model than the one used for control design, further work is needed to formally address the issue of robustness with respect to model uncertainty.

References

[1] M. A. Bolender and D. B. Doman, "Flight path angle dynamics of air-breathing hypersonic vehicles," AIAA Paper 2006-6692, 2006.

[2] J. T. Parker, A. Serrani, S. Yurkovich, M. A. Bolender, and D. B. Doman, "Control-oriented modeling of an air-breathing hypersonic vehicle," *Journal of Guidance, Control, and Dynamics*, vol. 30, no. 3, pp. 856–869, 2007.

[3] M. A. Bolender and D. B. Doman, "A nonlinear longitudinal dynamical model of an air-breathing hypersonic vehicle," *Journal of Spacecraft and Rockets*, vol. 44, no. 2, pp. 374–387, 2007.

[4] L. Fiorentini, A. Serrani, M. A. Bolender, and D. B. Doman, "Robust nonlinear sequential loop closure control design for an air-breathing hypersonic vehicle model," in *Proceedings of the 2008 American Control Conference*, Seattle, WA, 2008.

[5] ——, "Nonlinear control of a hypersonic vehicle with structural flexibility," in *Proceedings of the 47th IEEE Conference on Decision and Control*, Cancun, Mexico, 2008.

[6] ——, "Nonlinear robust adaptive control of flexible air-breathing hypersonic vehicles," *Journal of Guidance, Control, and Dynamics*, vol. 32, no. 2, pp. 402–417, 2009.

[7] A. Isidori, L. Marconi, and A. Serrani, *Robust Autonomous Guidance: An Internal Model-Based Approach*, ser. Advances in Industrial Control. London, UK: Springer Verlag, 2003.

[8] E. Sontag, "On the input-to-state stability property," *European Journal of Control*, vol. 1, no. 1, pp. 24–36, 1995.

[9] A. R. Teel, "A nonlinear small gain theorem for the analysis of control systems with saturation," *IEEE Transactions on Automatic Control*, vol. 41, no. 9, pp. 1256–70, 1996.

[10] H. K. Khalil, *Nonlinear systems*. Upper Saddle River, N.J.: Prentice Hall, 2002.